

UC Berkeley

UC Berkeley Previously Published Works

Title

Negative transference numbers in poly(ethylene oxide)-based electrolytes

Permalink

<https://escholarship.org/uc/item/2630j6bs>

Journal

Journal of the Electrochemical Society, 164(11)

ISSN

0013-4651

Authors

Pesko, DM
Timachova, K
Bhattacharya, R
et al.

Publication Date

2017

DOI

10.1149/2.0581711jes

Peer reviewed



Negative Transference Numbers in Poly(ethylene oxide)-Based Electrolytes

Danielle M. Pesko,^{a,b} Ksenia Timachova,^{a,b} Rajashree Bhattacharya,^a Mackensie C. Smith,^{c,d} Irune Villaluenga,^{d,e} John Newman,^{a,b,*} and Nitash P. Balsara^{a,b,d,e,**,z}

^aDepartment of Chemical and Biomolecular Engineering, University of California, Berkeley, California 94720, USA

^bEnvironmental Energy Technology Division, Lawrence Berkeley National Laboratory, Berkeley, California 94720, USA

^cDepartment of Materials Science and Engineering, University of California, Berkeley, California 94720, USA

^dMaterials Science Division, Lawrence Berkeley National Laboratory, Berkeley, California 94720, USA

^eJoint Center for Energy Storage Research (JCESR), Lawrence Berkeley National Laboratory, Berkeley, California 94720, USA

The performance of battery electrolytes depends on three independent transport properties: ionic conductivity, diffusion coefficient, and transference number. While rigorous experimental techniques for measuring conductivity and diffusion coefficients are well-established, popular techniques for measuring the transference number rely on the assumption of ideal solutions. We employ three independent techniques for measuring transference number, t_+ , in mixtures of polyethylene oxide (PEO) and lithium bis(trifluoromethanesulfonyl) imide (LiTFSI) salt. Transference numbers obtained using the steady-state current method pioneered by Bruce and Vincent, $t_{+,SS}$, and those obtained by pulsed-field gradient NMR, $t_{+,NMR}$, are compared against a new approach detailed by Newman and coworkers, $t_{+,Ne}$, for a range of salt concentrations. The latter approach is rigorous and based on concentrated solution theory, while the other two approaches only yield the true transference number in ideal solutions. Not surprisingly, we find that $t_{+,SS}$ and $t_{+,NMR}$ are positive throughout the entire salt concentration range, and decrease monotonically with increasing salt concentration. In contrast, $t_{+,Ne}$ has a non-monotonic dependence on salt concentration and is negative in the highly-concentrated regime. Our work implies that ion transport in PEO/LiTFSI electrolytes at high salt concentrations is dominated by the transport of ionic clusters.

© The Author(s) 2017. Published by ECS. This is an open access article distributed under the terms of the Creative Commons Attribution 4.0 License (CC BY, <http://creativecommons.org/licenses/by/4.0/>), which permits unrestricted reuse of the work in any medium, provided the original work is properly cited. [DOI: 10.1149/2.058171jes] All rights reserved.



Manuscript submitted April 20, 2017; revised manuscript received June 28, 2017. Published July 13, 2017. *This paper is part of the JES Focus Issue on Mathematical Modeling of Electrochemical Systems at Multiple Scales in Honor of John Newman.*

Energy density and safety of conventional lithium-ion batteries is limited by the use of liquid electrolytes comprising mixtures of flammable organic solvents and lithium salts. Polymer electrolytes have the potential to address both limitations. However, the power and lifetime of batteries containing solvent-free polymer electrolytes remain inadequate for most applications. The performance of electrolytes in batteries depends on three independent transport properties: ionic conductivity, σ , salt diffusion coefficient, D , and cation transference number, t_+ .¹ The poor performance of batteries with polymer electrolytes is generally attributed to low conductivity, which is on the order of 10^{-3} S/cm at 90°C for mixtures of polyethylene oxide (PEO) and lithium bis(trifluoromethanesulfonyl) imide (LiTFSI) salt,^{2,3} compared to that of liquid electrolytes which is 10^{-2} S/cm at ambient temperatures.⁴ Much of the literature in this field has been devoted to increasing the ionic conductivity of these materials.⁵⁻³² The purpose of our work is to shed light on another transport property of polymer electrolytes, the transference number.

In a pioneering study, Ma and coworkers showed that the transference number of a mixture of PEO and a sodium salt is negative.³³ Following this approach, others have obtained $t_+ < 0$ in polymers containing lithium or sodium salts.³⁴⁻³⁶ Nevertheless, the majority of reports for t_+ in polymer electrolytes fall between zero and one.³⁷⁻⁵¹ In contrast, all reports of t_+ in non-aqueous liquid electrolytes containing lithium salts fall between zero and one, including those that followed the techniques outlined by Ma and coworkers.⁵²⁻⁵⁶ Zugmann and coworkers presented a comparative study using four different methods for measuring t_+ in nonaqueous liquid electrolytes. In all cases, t_+ fell in the range of 0.25 to 0.35. Similar comprehensive studies of t_+ in polymer electrolytes have not yet been conducted. It is clear that more work is needed to clarify the value of t_+ in polymer electrolytes.

The most popular approach for estimating t_+ in polymer electrolytes is that developed by Bruce and Vincent.^{42,57} In this approach, the electrolyte of interest is sandwiched between two lithium electrodes, and the current, i , obtained under a fixed applied potential, ΔV , is monitored as a function of time, t . Bruce and Vincent showed that for electrolytes that exhibit ideal solution behavior

$$t_{+,SS} = \frac{i_{SS}}{i_0}, \quad [1]$$

where i_0 is the initial current, i_{SS} is the steady-state current, and the subscript SS in $t_{+,SS}$ indicates the approach used to obtain the transference number. It is now fairly routine to report both σ and $t_{+,SS}$ of newly-developed polymer electrolytes.^{41,44,45,47,48,58-60} The question of limits on i_{SS}/i_0 , or equivalently, $t_{+,SS}$ is an interesting open question. While most papers have reported i_{SS}/i_0 values between 0 and 1, there is at least one report wherein i_{SS}/i_0 obtained from an electrolyte was greater than 1.⁶¹ Since there are no bounds on the value of t_+ , Eq. 1 suggests that there may be no bounds on i_{SS}/i_0 .

In more recent work by Newman and coworkers,^{62,63} it was shown that for concentrated electrolytes,

$$\frac{i_{SS}}{i_0} = \frac{1}{1 + Ne}, \quad [2]$$

where

$$Ne = a \frac{\sigma RT (1 - t_{+,Ne})^2}{F^2 Dc} \left(1 + \frac{d \ln \gamma_{\pm}}{d \ln m} \right). \quad [3]$$

Here R is the gas constant, T is the temperature, F is Faraday's constant and c is the bulk concentration of the electrolyte. The parameter a is related to the stoichiometry of the salt, which is equal to 2 for monovalent salts such as LiTFSI. The thermodynamic factor, $1 + d \ln \gamma_{\pm} / d \ln m$, quantifies the change in the mean molal activity coefficient of the salt, γ_{\pm} , with the molality, m , of the solution. Measurements of i_{SS}/i_0 , σ , D , and $1 + d \ln \gamma_{\pm} / d \ln m$ are combined to obtain $t_{+,Ne}$. Note that all of the

*Electrochemical Society Fellow.

**Electrochemical Society Member.

^zE-mail: nbalsara1@gmail.com

terms on the right side of Eq. 3 are positive. This indicates that i_{ss}/i_0 must lie between zero and one, regardless of the magnitude or sign of t_+ (See Eq. 2); measurements outside this range must be affected by side reactions or some other artifact. It was shown in Reference 63 that Eq. 3 reduces to Eq. 1 in the limit of infinitely-dilute ideal solutions.

Complimentary information can be obtained by ^7Li and ^{19}F pulsed-field gradient NMR experiments. These experiments enable determination of the self-diffusion coefficients of species containing Li and F, D_{Li} and D_{F} . For fully dissociated electrolytes, D_{Li} represents the diffusion coefficient of the cation while D_{F} represents the diffusion coefficient of the anion. It is customary to define a transference number based on NMR as

$$t_{+,NMR} = \frac{D_{\text{Li}}}{D_{\text{Li}} + D_{\text{F}}} \quad [4]$$

The purpose of this paper is to report on the dependence of $t_{+,SS}$, $t_{+,Ne}$, and $t_{+,NMR}$ on salt concentration in mixtures of PEO and LiTFSI, a standard polymer electrolyte. It is important to recognize that the transference number required for modeling battery performance¹ is $t_{+,Ne}$, not $t_{+,SS}$ nor $t_{+,NMR}$.

Experimental

Electrolyte preparation and density measurements.—Electrolytes were prepared according to the procedures outlined in Reference 64. All electrolytes are homogeneous mixtures of 5 kg/mol PEO with $-\text{OH}$ endgroups (Polymer Source) and lithium bis(trifluoromethanesulfonyl)imide (LiTFSI) salt (Novalyte). Electrolytes are prepared at varying salt concentrations, ranging from $r = 0.01$ to $r = 0.3$, where $r = [\text{Li}^+]/[\text{O}]$ is the molar ratio of lithium ions to ether oxygens.

The density, ρ , at each salt concentration was obtained by measuring the mass of electrolyte within a known volume at 90°C . Results are shown in Table I, where the reported density is based on a single measurement due to limited sample. We measured neat PEO density three times and found the standard deviation to be about 2%. We take this to be the error for all of our measurements.

Salt concentration, c , was calculated from r and ρ according to

$$c = \frac{\rho r}{M_{\text{EO}} + r M_{\text{salt}}} \quad [5]$$

where M_{EO} is the molar mass of the ethylene oxide repeat unit (44.05 g/mol) and M_{LiTFSI} is the molar mass of LiTFSI (287.09 g/mol). The molality of the electrolyte, m , is calculated according to

$$m = \frac{r}{M_{\text{EO}}} \quad [6]$$

Table I provides values of ρ , c , and m for all electrolytes in this study.

Table I. Measured values of density and calculated values of salt concentration (Eq. 5) and molality (Eq. 6) for each electrolyte based on r .

r	ρ (g/L)	c (mol/L)	m (mol/kg)
0.00	1128	0.00	0.00
0.01	1160	0.25	0.23
0.02	1180	0.47	0.45
0.04	1210	0.87	0.91
0.06	1230	1.20	1.36
0.08	1330	1.59	1.81
0.10	1365	1.87	2.27
0.12	1380	2.11	2.72
0.14	1430	2.38	3.17
0.16	1450	2.58	3.63
0.30	1640	3.78	6.80

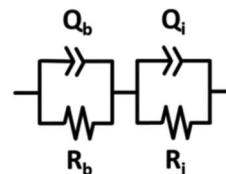


Figure 1. Equivalent electrical circuit for a symmetric cell with non-blocking electrodes. This circuit was fit to ac impedance spectroscopy data to obtain bulk resistance, R_b , and interfacial resistance, R_i , of the cell.

Electrochemical characterization.—All sample preparation was performed inside of an argon glovebox (MBraun) in order to maintain water and oxygen levels below 1 and 5 ppm respectively. Conductivity samples were prepared according to the procedures outlined in Reference 64. Lithium symmetric cells were prepared for steady-state current and restricted diffusion measurements of the electrolytes. Samples were made by pressing the polymer electrolyte into a 508 μm thick silicone spacer and sandwiching between two 150 μm thick lithium foils (MTI Corporation) backed with nickel foil. A stainless-steel shim was placed on either side of the sample to prevent the sample from deforming, which could lead to a change in electrolyte thickness or a cell short. Nickel tabs were secured to the stainless-steel shims to serve as electrical contacts. The assembly was vacuum sealed in a laminated aluminum pouch material (Showa-Denko) before removal from the glovebox. All samples were annealed at 90°C for 4 hours prior to electrochemical characterization.

Steady-state current and restricted diffusion measurements were performed using a Biologic VMP3 potentiostat. All measurements were performed at 90°C . At the beginning of the experiment, cells were conditioned for 5 charge/discharge cycles at a low current density of 0.02 mA/cm^2 to ensure a stable interfacial layer was introduced. Each conditioning cycle consisted of a 4 h charge followed by a 45 min rest and a 4 h discharge. Ac impedance spectroscopy was performed prior to potentiostat polarization. Complex impedance measurements were acquired for a frequency range of 1 MHz to 1 Hz at an amplitude of 80 mV. The data were analyzed in the form of a Nyquist plot and fit to an equivalent electrical circuit suitable for a symmetric cell with non-blocking electrodes. This circuit is shown in Figure 1, where Q_b and Q_i are the bulk and interfacial pseudo-capacitance, and R_b and R_i are the bulk and interfacial resistance of the cell. During the steady-state current experiment, current was measured at time intervals of 5 s while the cell was polarized for 4 h, long enough to reach a steady-state current. Potentials of $\Delta V = 10 \text{ mV}$, -10 mV , 20 mV , and -20 mV were used to ensure that the ion transport characteristics were independent of the sign and magnitude of the applied potential. Each data point in this study represents an average of all applied potentials. The cell resistances were measured as a function of time by performing ac impedance spectroscopy every 20 minutes during polarization. Here, the center of the ac input signal was offset by ΔV , and the amplitude was set to 10 mV to minimize disturbance of the polarization signal.

In the absence of a concentration gradient, current is defined by Ohm's law,

$$i_\Omega = \frac{\Delta V}{R_{i,0} + R_{b,0}} \quad [7]$$

where ΔV is the applied potential and $R_{i,0}$ and $R_{b,0}$ are cell resistances measured by ac impedance spectroscopy prior to polarization.⁴¹

The steady-state current experiment is used to determine the transference number defined by the work of Bruce and Vincent,^{42,57}

$$t_{+,SS} = \frac{i_{SS}(\Delta V - i_\Omega R_{i,0})}{i_\Omega(\Delta V - i_{SS} R_{i,SS})} \quad [8]$$

where ΔV is the applied potential, i_Ω is the initial current calculated according to Eq. 7, i_{SS} is the current measured at steady-state, and $R_{i,0}$

and $R_{i,SS}$ are the initial and steady-state resistances of the interface, respectively.

Restricted diffusion measurements are performed using the polarization induced by the steady-state current experiment. The applied potential was removed, and the cells were allowed to relax for 2 h while the open-circuit voltage, U , was measured at time intervals of 5 s. The salt diffusion coefficient, D , is calculated using

$$-\frac{d \ln U}{dt} = \frac{\pi^2 D}{L^2}, \quad [9]$$

where the left side of the equation is the slope from the least-squares fit of $-\ln U$ vs. time from $t = 5$ min to $t = 2$ h. We exclude $t = 0$ to 5 min to allow the electric double layer to discharge fully prior to the diffusion measurement. L is the final thickness of the electrolyte, which is measured after the completion of all electrochemical measurements.

Concentration cells were prepared using a similar cell configuration as that described in Reference 33 with a diffusion length of several centimeters to prevent the concentration gradient from relaxing too quickly. Unlike the solid electrolyte films described in previous reports,³³⁻³⁷ the electrolytes in this study were contained within a spacer to prevent leakage at high temperatures. A channel approximately 3 cm long and 2 mm wide was cut in a 508 μm thick silicone spacer. Half of the channel was filled with reference electrolyte ($r_{\text{ref}} = 0.06$), and the other half was filled with electrolytes at various r . Lithium electrodes backed with nickel foil were placed on either end of the channel. Nickel tabs were secured to the nickel foil, and the assembly was vacuum sealed in a laminated aluminum pouch material. Each cell was annealed at 90°C for 20 hours before the open-circuit voltage, U , was measured using a Biologic VMP3 potentiostat. Two or three concentration cells were prepared for each salt concentration.

Measurements of σ , D , and $t_{+,SS}$, were combined with the concentration cell data to calculate $t_{+,Ne}$. For both stainless-steel and lithium symmetric cells (σ , D , and $t_{+,SS}$), three samples were prepared, the measurements were averaged, and the standard deviation is reported as the error ($\delta\sigma$, δD , and $\delta t_{+,SS}$). The error for $t_{+,Ne}$, $\delta t_{+,Ne}$, is propagated according to

$$\delta t_{+,Ne} = |t_{+,Ne}| \sqrt{\left(\frac{\delta D}{D}\right)^2 + \left(\frac{\delta\sigma}{\sigma}\right)^2 + \left(\frac{\delta t_{+,SS}}{t_{+,SS}}\right)^2}. \quad [10]$$

Typical values for $\delta D/D$ fell in the range of 0.05 to 0.37, $\delta\sigma/\sigma$ fell in the range of 0.03 to 0.36, and $\delta t_{+,SS}/t_{+,SS}$ fell in the range of 0.02 to 0.20.

Determination of $t_{+,Ne}$ requires three independent measurements conducted using lithium/polymer cells: $t_{+,SS}$ and D from lithium symmetric cells and the thermodynamic factor from concentration cells. All of these could theoretically be influenced by the presence of the solid electrolyte interface (SEI) that forms spontaneously at the lithium-polymer interface. To address this issue, lithium symmetric cells are always conditioned prior to electrochemical measurements. These low-current polarizations are used to set up a stable lithium-polymer interface that does not change throughout the course of the measurements. The Bruce and Vincent measurement of $t_{+,SS}$ accounts for SEI formation, as the time-dependence of the interfacial resistance is accounted for in the calculation (see Equation 8). In the experiments reported here there is no change in either bulk or interfacial impedance during the $t_{+,SS}$ and D measurements. We deliberately chose to work with 500 μm thick samples to ensure that the potential relaxation in our restricted diffusion experiments is dominated by salt diffusion in the bulk (i.e. to minimize interfacial relaxation contributions). Concentration cells cannot be conditioned prior to the measurement as this may change the concentration gradient within the cells. We thus allowed for stable SEI formation by annealing the cells for 20 hours prior to measurement of the OCV. Between hours 0–20, the OCV of the cell varies with time, an observation that we attribute to interfacial reactions related to SEI formation. It is unclear at this point what role these SEI layers play in data obtained from the concentration cells.

The same limitation applies to all of the concentration cell data in the literature.

Pulsed-field gradient NMR (PFG-NMR) characterization.— Electrolytes were placed into NMR tubes and sealed with high pressure polyethylene caps before measurement. NMR measurements were performed on a Bruker Avance 600 MHz instrument fitted with a Z-gradient direct detection broad-band probe and a variable temperature unit maintained at 90°C throughout the experiments. Measurements were performed on the isotopes of ^7Li and ^{19}F to probe the diffusion of lithiated and fluorinated salt species, respectively. All samples produced peaks around 233 MHz for lithium and 565 MHz for fluorine corresponding to all lithium- and TFSI-containing ions. The 90° pulse lengths were optimized for each sample to achieve maximum signal amplitude. T1 relaxation times were independently measured for each sample nuclei using inversion-recovery (180- τ -90-acq.) to insure the choice of an appropriate diffusion time interval, Δ . A bipolar gradient pulse sequence was used to measure the self-diffusion coefficients, D_i . The attenuation of the echo E was fit to,

$$E = e^{-\gamma^2 g^2 \delta^2 D_i (\Delta - \frac{\delta}{3})} \quad [11]$$

where γ is the gyromagnetic ratio, g is the gradient strength, δ is the duration of the gradient pulse, Δ is the interval between gradient pulses, τ is the separation between pulses, and D_i is the self-diffusion coefficient. Parameters used for acquisition were diffusion intervals $\Delta = 0.55$ to 0.85 s (^7Li) and 0.96 to 1.2 s (^{19}F), and pulse lengths $\delta = 5$ to 10 ms (^7Li) and 1 to 2.5 ms (^{19}F). For each diffusion measurement, 32 experiments of varying gradient strength were performed, and the change in amplitude of the attenuated signal was fit to obtain the parameter D_i . All measured signal attenuations were single exponential decays, and R^2 values for all fits were greater than 0.99 for both ^{19}F and ^7Li . Only one data point was collected for each r value, because of the complexity and length of the PFG-NMR measurements at slow diffusion times.

Results and Discussion

We determine ionic conductivity, diffusion coefficient, and transference number in PEO/LiTFSI mixtures as a function of salt concentration using three separate experiments: ac impedance spectroscopy, restricted diffusion, and measurement of the steady-state current.

Ionic conductivity, σ , measured using ac impedance, is plotted as a function of salt concentration in Figure 2a. Here, salt concentration is expressed in terms of r , the molar ratio of lithium ions to ether oxygens. Figure 2a indicates that σ has a non-monotonic dependence on r , reaching a maximum of 2×10^{-3} S/cm at $r = 0.08$. This is in agreement with literature and the reason for this observation is well-established.^{2,3,64,65} At low salt concentrations, conductivity increases with increasing salt concentration due to an increase in the concentration of charged species. However, ion transport in polymer electrolytes is coupled to segmental motion, which slows down in the presence of salt due to interactions between ether oxygen atoms and lithium ions. This effect dominates conductivity at $r > 0.08$.

Figure 2b shows the salt diffusion coefficient, D , over the same range of salt concentrations, determined by restricted diffusion. We find that all measurements of D fall within the range of 5.8×10^{-8} to 1.3×10^{-7} cm²/s. The dependence of D on r appears to be complicated. At low salt concentrations, D increases with increasing r . At intermediate salt concentrations, D decreases with increasing r before increasing again in the vicinity of $r = 0.16$. D increases by a factor of 1.6 when r is increased from 0.14 to 0.16. Conductivity increases by a more modest factor of 1.3 in the same salt concentration range (Figure 2a). Qualitatively similar behavior was reported for PEO/NaTFSI mixtures in the same concentration range (PEO molecular weight = 5000 kg/mol).³⁴ In contrast, D of PEO/NaTf (sodium triflate) mixtures decreased monotonically with increasing r (PEO molecular weight = 5000 kg/mol).³³ To our knowledge, there are no

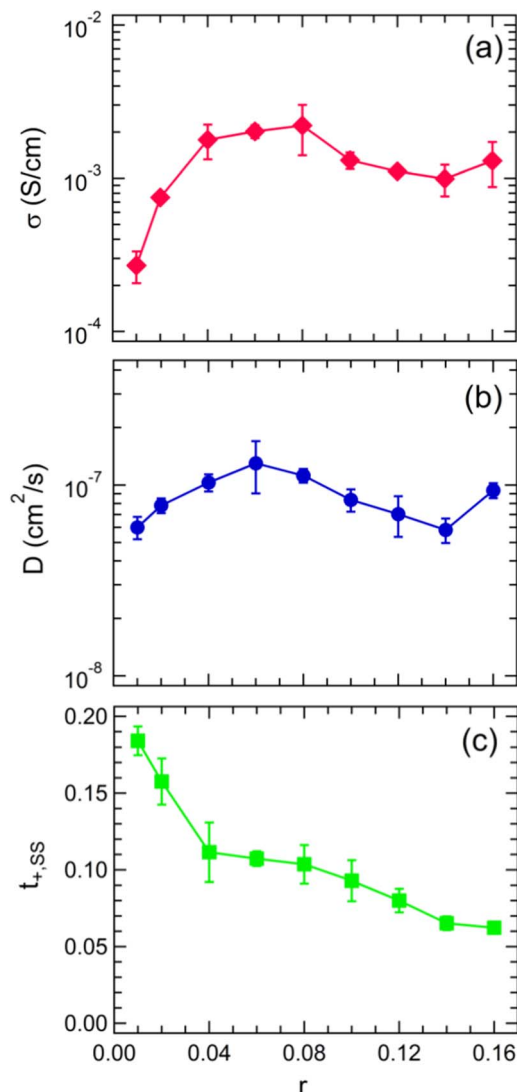


Figure 2. (a) Conductivity from ac impedance spectroscopy of symmetric cells with blocking electrodes. (b) Salt diffusion coefficient obtained by restricted diffusion in a lithium symmetric cell. (c) Transference number obtained using the steady-state current technique in a lithium symmetric cell. All data are for 5 kg/mol PEO with LiTFSI at 90°C.

published reports on the dependence of D on salt concentration in mixtures of PEO and LiTFSI. There are, however, three separate studies of D in PEO/LiTFSI mixtures at fixed salt concentrations. Mullin et al. reported $D = 1.1 \times 10^{-7} \text{ cm}^2/\text{s}$ for 27 kg/mol PEO at $r = 0.085$ and 90°C,⁶⁶ Edman et al. reported $D = 4.6 \times 10^{-8} \text{ cm}^2/\text{s}$ for 5,000 kg/mol PEO at $r = 0.083$ and 85°C,³⁷ and Geiculescu et al. reported $D = 4.2 \times 10^{-8} \text{ cm}^2/\text{s}$ for 4,000 kg/mol PEO at $r = 0.033$ and 90°C.⁵⁹ Our results are in agreement with that of Mullin et al. In contrast, D determined by Edman et al. and Geiculescu et al. are lower than those reported here. More work is needed to establish the dependence of D on polymer molecular weight and salt concentration.

Transference numbers measured by the steady-state current method, $t_{+,SS}$, are given in Figure 2c. We find that $t_{+,SS}$ decreases monotonically with increasing r , with a maximum value of 0.18 at $r = 0.01$ and a minimum of 0.06 at $r = 0.16$. Our values are in excellent agreement with a recent report of transference number in PEO/LiTFSI electrolytes measured using the steady-state current method.⁶⁰ Note that our value of $t_{+,SS}$ is based on the ratio i_{ss}/i_{Ω} rather than i_{ss}/i_0 , where i_0 is the experimentally determined initial current and i_{Ω} is the calculated initial current (see Experimental section).

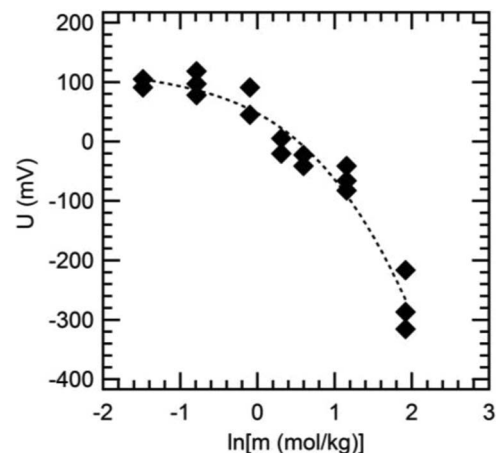


Figure 3. Measured open circuit potential, U , from concentration cells of the form $\text{Li} | \text{PEO/LiTFSI} (r_{\text{ref}}) | \text{PEO/LiTFSI} (r) | \text{Li}$ at 90°C. Here, r_{ref} is the reference held at $r = 0.06$, and r is varied. Each point represents data from one concentration cell. The dashed line shows the polynomial fit given by Eq. 13.

Combining Equations 1, 2, and 3 we obtain

$$t_{+,Ne} = 1 - \frac{F^2 D c \left(\frac{1}{t_{+,SS}} - 1 \right)}{\sqrt{a \sigma R T \left(1 + \frac{d \ln \gamma_{\pm}}{d \ln m} \right)}}, \quad [12]$$

Equation 12 indicates that four independent measurements must be performed in order to obtain the true transference number of an electrolyte: σ , D , $t_{+,SS}$, $1 + d \ln \gamma_{\pm} / d \ln m$. We have shown data for σ , D , and $t_{+,SS}$ as a function of r in Figure 2. Next, we focus on the measurement of $1 + d \ln \gamma_{\pm} / d \ln m$, often referred to as the thermodynamic factor in the literature, using concentration cells.

Concentration cells are of the form $\text{Li} | \text{PEO/LiTFSI} (r_{\text{ref}}) | \text{PEO/LiTFSI} (r) | \text{Li}$. The open circuit potential, U , of these cells was measured as a function of r with r_{ref} held fixed at 0.06. For consistency, we averaged values of U recorded between $t = 20$ h and $t = 25$ h in all of the experiments. The results of these experiments are shown in Figure 3; independent cells with the same nominal salt concentration exhibited slightly different values of U . We take U to be positive when $r < r_{\text{ref}}$ and negative when $r > r_{\text{ref}}$. The data in Figure 3 are consistent with those published by Edman et al. for mixtures of 5000 kg/mol PEO and LiTFSI.³⁷ The dependence of U on m is assumed to follow a power series of $\ln m$. The dashed line in Figure 3b shows the best fit polynomial equation of the form

$$U = 47.478 - 70.320 (\ln m) - 33.145 (\ln m)^2 - 8.052 (\ln m)^3 \quad [13]$$

where m has units of mol/kg and U is in mV. The important quantity is the derivative of Eq. 13, $dU/d \ln m$, because

$$\left(1 + \frac{d \ln \gamma_{\pm}}{d \ln m} \right) = - \frac{F}{2RT_{-}} \left(\frac{dU}{d \ln m} \right), \quad [14]$$

Our approach for measuring the thermodynamic factor is well established, and has been applied to a variety of systems including polymer electrolytes³³⁻³⁷ and liquid electrolytes.^{53,55,67}

Self-diffusion coefficients measured by ^7Li and ^{19}F pulsed-field gradient NMR (PFG-NMR) in our PEO/LiTFSI mixtures are shown in Figure 4. At all concentrations, the self-diffusion coefficient of the fluorine-containing species (D_F) is greater than that of the lithium-containing species (D_{Li}), consistent with previous reports in the literature for PFG-NMR in polymer electrolytes.^{38,50,68-70} Both self-diffusion coefficients decrease with increasing salt concentration. These measurements enable determination of $t_{+,NMR}$ as a function of r using Eq. 4.

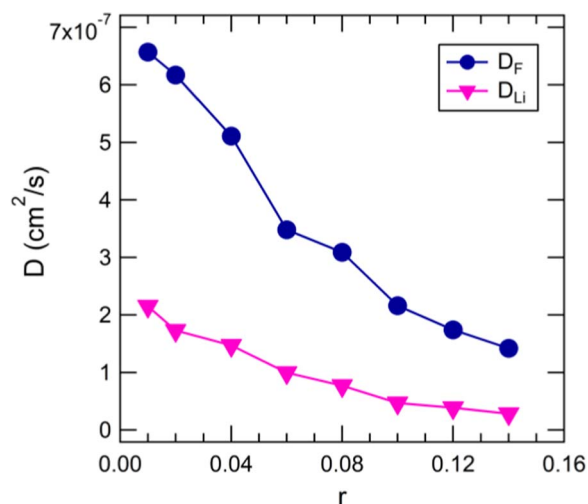


Figure 4. Self-diffusion coefficients for lithium-containing species, D_{Li} , and the fluorine-containing species, D_F , measured using PFG-NMR at 90°C.

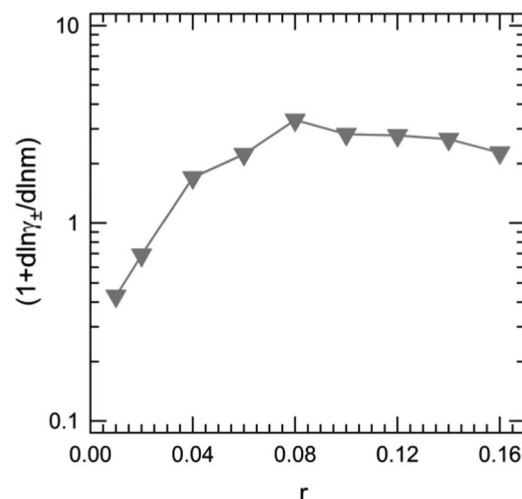


Figure 6. Thermodynamic factor for 5 kg/mol PEO with LiTFSI at 90°C as a function of salt concentration.

The difference in the dependence of self and mutual diffusion coefficients on salt concentration is noteworthy; compare Figures 2b and 4. The addition of salt is known to slow down segmental motion and this is expected to reduce the mobility of the ions, particularly that of the cations that are coordinated with the ether oxygens in PEO. It is evident that this effect dominates the measured self-diffusion coefficient (Figure 4). Mutual diffusion coefficients are, however, also affected by factors related to osmotic effects which depend on the state of dissociation of the salt. We attribute the non-monotonic dependence of the mutual diffusion coefficient on salt concentration to the fact that it is affected by more than one factor.

Results for $t_{+,SS}$, $t_{+,NMR}$ and $t_{+,Ne}$ as a function of r are shown in Figure 5. We find that $t_{+,NMR}$ and $t_{+,SS}$, values obtained using approaches that rely on ideal solution assumptions, are positive over the entire range of salt concentrations, and decrease monotonically with increasing r . In contrast, $t_{+,Ne}$ has a non-monotonic dependence on r . At high salt concentrations ($r \geq 0.12$), $t_{+,Ne}$ is negative, reaching a value as low as -0.38 at $r = 0.16$. There is also a significant difference between $t_{+,Ne}$ and $t_{+,SS}$ in the dilute limit at $r = 0.01$; while $t_{+,SS}$ is about 0.18 (and $t_{+,NMR}$ is about 0.25), $t_{+,Ne}$ is 0.07 (see Figure 5b). It is evident that the true transference number in PEO/LiTFSI mixtures

is very different from those obtained using approximate methods such as the Bruce-Vincent method and PFG-NMR.

For completeness, we use $t_{+,Ne}$ to calculate the thermodynamic factor, $1 + d \ln \gamma_{\pm} / d \ln m$, according to Eq. 14. The dependence of $1 + d \ln \gamma_{\pm} / d \ln m$ on salt concentration is shown in Figure 6. We find that $1 + d \ln \gamma_{\pm} / d \ln m$ has a non-monotonic dependence on r , reaching a maximum of 3.3 at $r = 0.08$. For ideal solutions, $\gamma_{\pm} = 1$, independent of salt concentration; thus, $d \ln \gamma_{\pm} / d \ln m = 0$ for ideal solutions. Our results suggest that PEO/LiTFSI mixtures are closest to ideal solutions in the vicinity of $r = 0.03$. It is interesting to note that there is agreement between the three different measurements of transference numbers near this concentration ($r = 0.02$, see Figure 5). In contrast, the most dilute PEO/LiTFSI mixture that we have studied, $r = 0.01$, is non-ideal. The underpinnings of this observation remain to be established. The value of $1 + d \ln \gamma_{\pm} / d \ln m$ at $r = 0.06$ reported by Georen and Lindbergh for PEO/LiTFSI (PEO molecular weight 5,000 kg/mol) at 85°C was approximately 12.⁷¹ This differs substantially from the value that we report (3.3 at $r = 0.08$). We also note that the transference number of this system was found to be positive at all salt concentrations.³⁷ It is not clear if differences in molecular weight are responsible for these differences.

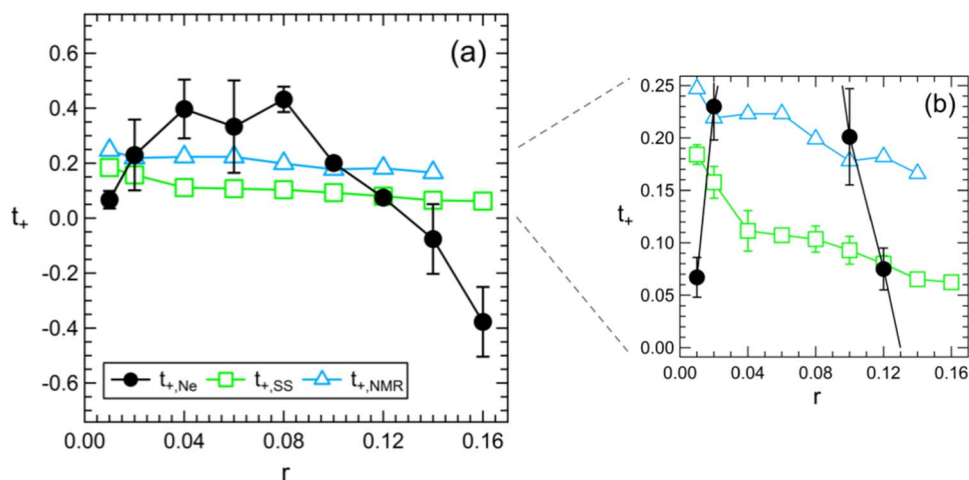


Figure 5. (a) Transference number, t_+ , for mixtures of PEO and LiTFSI at varying salt concentration, r , using three different methods: $t_{+,NMR}$ is obtained by PFG-NMR measurements of D_{Li} and D_F , and is calculated using Eq. 4; $t_{+,SS}$ is measured using the steady-state current method calculated using Eq. 8; $t_{+,Ne}$ combines measurements of conductivity, restricted diffusion, $t_{+,SS}$, and the thermodynamic factor and is calculated using Eq. 12. (b) Same data on an expanded scale.

Negative transference numbers indicate the presence of ion clusters such as charged triplets in addition to free cations and anions. All of the charged species in the electrolyte contribute to the measured transference number. If we assume that the electrolyte contains both cations (Li^+) and negatively-charged triplets ($\text{Li}(\text{TFSI})_2^-$), then negative transference numbers are obtained when ion transport is dominated by the negatively-charged triplets.³³ The presence of ion clusters in PEO/LiTFSI mixtures has been established by Raman spectroscopy.^{40,72} Both studies concluded that free ions are the dominant species at lower concentrations, but at $r > 0.125$ ion pairs or aggregates are present. Interestingly, this concentration is where $t_{+, \text{Ne}}$ changes sign (Figure 5). Further studies are needed to establish the underpinnings of negative transference numbers in polymer electrolytes.

Conclusions

We employ a new approach for determining the transference number of polymer electrolytes. It is based on the measurement of conductivity by ac impedance, salt diffusion coefficient by restricted diffusion, steady-state current under dc polarization, and the thermodynamic factor using concentration cells. Our approach, based on concentrated solution theory, is very similar to that proposed by Ma et al.³³ A majority of t_+ values reported in the literature^{41–45,47–49,58,59,61} are based on the steady-state current method pioneered by Bruce and Vincent.^{42,57} In a few cases^{34–37} where the approach of Ma et al. is used to determine t_+ , there is no attempt to relate t_+ values thus obtained with those that might be obtained using the steady-state current method. This paper provides a bridge between these two distinct approaches.

We report measurements of t_+ in mixtures of PEO and LiTFSI using the steady-state current method, $t_{+, \text{SS}}$, pulsed-field gradient NMR, $t_{+, \text{NMR}}$, and the present approach, $t_{+, \text{Ne}}$, for a range of salt concentrations. We find that methods that rely on ideal solution assumptions ($t_{+, \text{SS}}$ and $t_{+, \text{NMR}}$) yield positive values for t_+ falling within the narrow range of $0.06 < t_{+, \text{SS}} < 0.18$ and $0.17 < t_{+, \text{NMR}} < 0.25$. Both transference numbers decrease monotonically with increasing salt concentration. In contrast, $t_{+, \text{Ne}}$ has a non-monotonic dependence on salt concentration with a peak at intermediate salt concentrations ($r = 0.08$). In addition, $t_{+, \text{Ne}}$ is negative at high salt concentrations ($r \geq 0.12$), reaching a value as low as -0.38 at $r = 0.16$. Our work implies that charged triplets are likely to be the dominant species in PEO/LiTFSI electrolytes in the highly-concentrated regime. Further studies are needed to characterize the nature of the speciation in this system.

Acknowledgments

The work reported here was supported by the National Science Foundation grant NSF-CHE-1333736 in the Designing Materials to Revolutionize and Engineer our Future Program. The authors declare no competing financial interest.

List of Symbols

a	stoichiometric parameter
c	salt concentration (mol/L)
D	salt diffusion coefficient (cm^2/s)
D_{F}	self-diffusion coefficients of the species containing F (cm^2/s)
D_{i}	self-diffusion coefficient (cm^2/s)
D_{Li}	self-diffusion coefficients of the species containing Li (cm^2/s)
E	attenuation of the echo
F	Faraday's constant (96485 C/mol)
g	gyromagnetic ratio
i	current density (mA/cm^2)
i_0	initial current (mA/cm^2)

i_{ss}	steady-state current (mA/cm^2)
L	thickness of the electrolyte (508 μm)
LiTFSI	lithium bis(trifluoromethanesulfonyl) imide
M_{EO}	molar mass of the ethylene oxide repeat unit (44.05 g/mol)
M_{LiTFSI}	molar mass of LiTFSI (287.09 g/mol)
m	molality (mol/kg)
Ne	dimensionless number defined by Equation 3
PEO	polyethylene oxide
Q_{b}	bulk capacitance (F)
Q_{i}	interfacial capacitance (F)
R	gas constant (J/mol K)
R_{b}	bulk resistance ($\Omega \text{ cm}^2$)
$R_{\text{b},0}$	initial bulk resistance ($\Omega \text{ cm}^2$)
R_{i}	interfacial resistance ($\Omega \text{ cm}^2$)
$R_{\text{i},0}$	initial interfacial resistance ($\Omega \text{ cm}^2$)
$R_{\text{i,SS}}$	steady-state interfacial resistance ($\Omega \text{ cm}^2$)
r	moles of Li^+ per mole of ethylene oxide
r_{ref}	concentration of reference electrolyte used in concentration cells
T	temperature (K)
t	time (h)
t_+	cation transference number
$t_{+, \text{Ne}}$	transference number obtained using Balsara and Newman method ⁶³
$t_{+, \text{NMR}}$	transference number obtained using pulsed-field gradient NMR
$t_{+, \text{SS}}$	transference number obtained using steady-state current method
U	open-circuit voltage (mV)
$1 + d \ln \gamma_{\pm} / d \ln m$	thermodynamic factor

Greek

γ_{\pm}	mean molal activity coefficient of the salt
Δ	duration of the gradient pulse (s)
ΔV	applied potential (mV)
δ	interval between gradient pulses (s)
ρ	density of the electrolyte (g/L)
σ	ionic conductivity (S/cm)
τ	separation between pulses (s)

References

- J. Newman and K. E. Thomas-Alyea, *Electrochemical Systems*, John Wiley & Sons, (2012).
- S. Lascaud, M. Perrier, A. Vallee, S. Besner, J. Prud'homme, and M. Armand, *Macromolecules*, **27**, 7469 (1994).
- A. A. Teran, M. H. Tang, S. A. Mullin, and N. P. Balsara, *Solid State Ionics*, **203**, 18 (2011).
- K. Xu, *Chem. Rev.*, **104**, 4303 (2004).
- K. Nagaoka, H. Naruse, I. Shinohara, and M. Watanabe, *J. Polym. Sci. Polym. Lett. Ed.*, **22**, 659 (1984).
- A. Nishimoto, M. Watanabe, Y. Ikeda, and S. Kohjiya, *Electrochim. Acta*, **43**, 1177 (1998).
- M. Watanabe, T. Endo, A. Nishimoto, K. Miura, and M. Yanagida, *J. Power Sources*, **81–82**, 786 (1999).
- A. Nishimoto, K. Agehara, N. Furuya, T. Watanabe, and M. Watanabe, *Macromolecules*, **32**, 1541 (1999).
- Y. Matoba, *Solid State Ionics*, **147**, 403 (2002).
- J. Acosta, *Solid State Ionics*, **85**, 85 (1996).
- B. K. Choi, Y. W. Kim, and H. K. Shin, *Electrochim. Acta*, **45**, 1371 (2000).
- Z. Zhang, J. Jin, F. Bautista, L. Lyons, N. Shariatizadeh, D. Sherlock, K. Amine, and R. West, *Solid State Ionics*, **170**, 233 (2004).
- M. Watanabe, *Solid State Ionics*, **148**, 399 (2002).
- F. Croce, L. Persi, B. Scrosati, F. Serraino-Fiory, E. Plichta, and M. A. Hendrickson, *Electrochim. Acta*, **46**, 2457 (2001).
- P. Johansson, M. A. Ratner, and D. F. Shriver, *J. Phys. Chem. B*, **105**, 9016 (2001).
- K. R. Baldwin, A. J. Golder, and J. Knight, *Royal Aircraft Establishment, Report no. 84036* (1984).
- C. S. Harris, D. F. Shriver, and M. A. Ratner, *Macromolecules*, **19**, 987 (1986).
- T. Morioka, K. Ota, and Y. Tominaga, *Polymer (Guildf)*, **84**, 21 (2016).

19. M. Smith, M. Silva, S. Cerqueira, and J. R. MacCallum, *Solid State Ionics*, **140**, 345 (2001).
20. R. D. Armstrong and M. D. Clarke, *Electrochim. Acta*, **29**, 1443 (1984).
21. R. Dupon, *J. Electrochem. Soc.*, **131**, 586 (1984).
22. M. Watanabe, M. Rikukawa, K. Sanui, N. Ogata, H. Kato, T. Kobayashi, and Z. Ohtaki, *Macromolecules*, **17**, 2902 (1984).
23. M. Watanabe, M. Togo, K. Sanui, N. Ogata, T. Kobayashi, and Z. Ohtaki, *Macromolecules*, **17**, 2908 (1984).
24. Y. Lee, M. A. Ratner, and D. F. Shriver, *Solid State Ionics*, **138**, 273 (2001).
25. K. P. Barteau, M. Wolffs, N. A. Lynd, G. H. Fredrickson, E. J. Krarner, and C. J. Hawker, *Macromolecules*, **46**, 8988 (2013).
26. J. M. G. Cowie and A. C. S. Martin, *Polymer (Guildf)*, **28**, 627 (1987).
27. M. Nekoomanesh, H. S. Nagae, C. Booth, and J. R. Owen, *J. Electrochem. Soc.*, **139**, 3046 (1992).
28. P. Blonsky, D. Shriver, P. Austin, and H. Allcock, *Solid State Ionics*, **18–19**, 258 (1986).
29. R. Hooper, L. J. Lyons, D. A. Moline, and R. West, *Organometallics*, **18**, 3249 (1999).
30. R. Hooper, L. J. Lyons, M. K. Mapes, D. Schumacher, D. A. Moline, and R. West, *Macromolecules*, **34**, 931 (2001).
31. M. Watanabe, S. Nagano, K. Sanui, and N. Ogata, *Solid State Ionics*, **18–19**, 338 (1986).
32. J. M. Sarapas and G. N. Tew, *Macromolecules*, **49**, 1154 (2016).
33. Y. Ma, M. Doyle, T. F. Fuller, M. M. Doeff, L. C. D. Jonghe, and J. Newman, *Electrochem. Soc.*, **142**, 1859 (1995).
34. A. Ferry, M. M. Doeff, and L. C. De Jonghe, *J. Electrochem. Soc.*, **145**, 1586 (1998).
35. A. Ferry, M. M. Doeff, and L. C. DeJonghe, *Electrochim. Acta*, **43**, 1387 (1998).
36. M. M. Doeff, P. Georén, J. Qiao, J. Kerr, and L. C. De Jonghe, *J. Electrochem. Soc.*, **146**, 2024 (1999).
37. L. Edman, M. M. Doeff, A. Ferry, J. Kerr, and L. C. De Jonghe, *J. Phys. Chem. B*, **104**, 3476 (2000).
38. S. Bhattacharja, S. Smoot, and D. Whitmore, *Solid State Ionics*, **18–19**, 306 (1986).
39. W. Gorecki, M. Jeannin, E. Belorizky, C. Roux, and M. Armand, *J. Phys. Condens. Matter*, **7**, 6823 (1995).
40. I. Rey, J. C. Lassègues, J. Grondin, and L. Servant, *Electrochim. Acta*, **43**, 1505 (1998).
41. M. Chintapalli, K. Timachova, K. R. Olson, S. J. Mecham, D. Devaux, J. M. DeSimone, and N. P. Balsara, *Macromolecules*, **49**, 3508 (2016).
42. J. Evans, C. A. Vincent, and P. G. Bruce, *Polymer (Guildf)*, **28**, 2324 (1987).
43. P. G. Bruce, J. Evans, and C. A. Vincent, *Solid State Ionics*, **28**, 918 (1988).
44. Y. Tominaga and K. Yamazaki, *Chem. Commun.*, **50**, 4448 (2014).
45. Y. Tominaga, K. Yamazaki, and V. Nanthana, *J. Electrochem. Soc.*, **162**, A3133 (2015).
46. Y. Tominaga, T. Shimomura, and M. Nakamura, *Polymer (Guildf)*, **51**, 4295 (2010).
47. M. Watanabe, S. Nagano, K. Sanui, and N. Ogata, *Solid State Ionics*, **28**, 911 (1988).
48. Y. Kato, M. Watanabe, K. Sanui, and N. Ogata, *Solid State Ionics*, **40**, 632 (1990).
49. D. H. C. Wong, J. L. Thelen, Y. Fu, D. Devaux, A. A. Pandya, V. S. Battaglia, N. P. Balsara, and J. M. DeSimone, *Proc. Natl. Acad. Sci. U. S. A.*, **111**, 3327 (2014).
50. K. Timachova, H. Watanabe, and N. P. Balsara, *Macromolecules*, **48**, 7882 (2015).
51. B. Sun, J. Mindemark, E. V. Morozov, L. T. Costa, M. Bergman, P. Johansson, Y. Fang, I. Furó, and D. Brandell, *Phys. Chem. Chem. Phys.*, **18**, 9504 (2016).
52. C. Capiglia, Y. Saito, H. Kageyama, P. Mustarelli, T. Iwamoto, T. Tabuchi, and H. Tukamoto, *J. Power Sources*, **81**, 859 (1999).
53. L. O. Valøen and J. N. Reimers, *J. Electrochem. Soc.*, **152**, A882 (2005).
54. J. Zhao, L. Wang, X. He, C. Wan, and C. Jiang, *J. Electrochem. Soc.*, **155**, A292 (2008).
55. S. Zugmann, M. Fleischmann, M. Amereller, R. M. Gschwind, H. D. Wiemhöfer, and H. J. Gores, *Electrochim. Acta*, **56**, 3926 (2011).
56. Y. Aihara, T. Bando, H. Nakagawa, H. Yoshida, K. Hayamizu, E. Akiba, and W. S. Price, *J. Electrochem. Soc.*, **151**, A119 (2004).
57. P. G. Bruce and C. A. Vincent, *J. Electroanal. Chem. Interfacial Electrochem.*, **225**, 1 (1987).
58. G. Jo, H. Jeon, and M. J. Park, *ACS Macro Lett.*, **4**, 225 (2015).
59. O. E. Geiculescu, R. Rajagopal, S. E. Creager, D. D. DesMarteau, X. Zhang, and P. Fedkiw, *J. Phys. Chem. B*, **110**, 23130 (2006).
60. K. Pożyczka, M. Marzantowicz, J. R. Dygas, and F. Krok, *Electrochim. Acta*, **227**, 127 (2017).
61. Y. Lu, M. Tikekar, R. Mohanty, K. Hendrickson, L. Ma, and L. Archer, *Adv. Energy Mater.*, **5**, 1402073 (2015).
62. M. Doyle and J. Newman, *J. Electrochem. Soc.*, **142**, 3465 (1995).
63. N. P. Balsara and J. Newman, *J. Electrochem. Soc.*, **162**, A2720 (2015).
64. D. M. Pesko, M. A. Webb, Y. Jung, Q. Zheng, T. F. Miller III, G. W. Coates, and N. P. Balsara, *Macromolecules*, **49**, 5244 (2016).
65. D. Devaux, R. Bouchet, D. Glé, and R. Denoyel, *Solid State Ionics*, **227**, 119 (2012).
66. D. M. Pesko, Y. Jung, A. L. Hasan, M. A. Webb, G. W. Coates, T. F. Miller III, and N. P. Balsara, *Solid State Ionics*, **289**, 118 (2016).
67. S. A. Mullin, G. M. Stone, A. Panday, and N. P. Balsara, *J. Electrochem. Soc.*, **158**, A619 (2011).
68. S. Stewart and J. Newman, *J. Electrochem. Soc.*, **155**, A458 (2008).
69. H. Hafezi and J. Newman, *J. Electrochem. Soc.*, **147**, 3036 (2000).
70. G. Örædd, L. Edman, and A. Ferry, *Solid State Ionics*, **152**, 131 (2002).
71. W. Gorecki, M. Jeannin, E. Belorizky, C. Roux, and M. Armand, *J. Phys. Condens. Matter*, **7**, 6823 (1995).
72. P. Georén and G. Lindbergh, *Electrochim. Acta*, **47**, 577 (2001).